WATER RESOURCES RESEARCH, VOL. 29, NO. 2, PAGES 293–303, FEBRUARY 1993

Spring Climate and Salinity in the San Francisco Bay Estuary

DANIEL R. CAYAN

U.S. Geological Survey, Scripps Institution of Oceanography, La Jolla, California

DAVID H. PETERSON

U.S. Geological Survey, Menlo Park, California

Salinity in the San Francisco Bay Estuary almost always experiences its yearly maximum during late summer, but climate variability produces marked interannual variations. The atmospheric circulation pattern impacts the estuary primarily through variations of runoff from rainfall and snowmelt from the Sierra Nevada and, secondarily, through variations in the near-surface salinity in the coastal ocean. While winter precipitation is the primary influence upon salinity in the estuary, spring climate variations also contribute importantly to salinity fluctuations. Spring atmospheric circulation influences both the magnitude and the timing of freshwater flows, through anomalies of precipitation and temperature. To help discriminate between the effects of these two influences, the record is divided into subsets according to whether spring conditions in the region are cool and wet, warm and wet, cool and dry, or warm and dry. Warm springs promote early snowmelt-driven flows, and cool springs result in delayed flows. In addition to effects of winter and spring climate variability operating on the watershed, there are more subtle effects that are transmitted into the estuary from the coastal ocean. These influences are most pronounced in cool and dry springs with high surface salinity (SS) in the coastal ocean versus cool and wet springs with low SS in the coastal ocean. A transect of SS records at stations from the mouth to the head of the bay suggests that the coastal ocean anomaly signal is attenuated from the mouth to the interior of the estuary. In contrast, a delayed, postsummer signal caused by winter and spring runoff variations from the upstream watershed are most pronounced at the head of the estuary and attenuate toward the mouth.

INTRODUCTION

The current 6-year drought in California and Nevada has brought regional water management problems to the forefront with a diminished freshwater supply and a degraded water quality of some of the state's water stock. A focal point of these problems is California's San Francisco Bay, Sacramento/San Joaquin River Delta, one of the largest estuaries of western North America. The bay is the outlet of the major watershed in the state. Through its inland delta it supplies fresh water to two thirds of the state's population [*U.S. Bureau of Reclamation,* 1987; *California State Water Resources Control Board,* 1991] and to one of the richest irrigated agricultural resources in the world [*Scheuring,* 19831. Understanding the bay's salinity variability, including natural and artificial controls on seasalt penetration, is fundamental to an understanding of its physics, chemistry, and ecology and for managing the freshwater flows and the biological resources dependent on them [*Nichols et al.,* 1986; *Cloern and Nichols,* 1985; *Conomos*, 1979]. For example, when the mountain snow-fed flow into the bay recedes to its lowest level in late summer-early fall, salt in the estuary reaches toward the delta with its greatest landward extent, threatens freshwater supplies [*U.S. Bureau of Reclamation,* 1987; *California State Water Resources Control Board,* 19911, and shifts sediment dynamics [*Siegfried et al.,* 1980]. High salinity in the bay favors an increasing population of marine filter-feeding benthic clams [*Nichols,* 1985] that can suppress phytoplankton biomass [*Nichols,* 1985; *Cloern,* 1982], thereby changing water chemistry [*Peterson et al.,* 1989] and food web dynamics [*Nichols,* 1985; *Carlton et al.,* 19901. Thus, as with many temperate zone estuaries, controls on the location and amplitude of the late summer salinity intrusion are especially important in times of drought.

Paper number 92WR02152.

SETTING

Overall, the greatest control on mean monthly surface salinity fluctuations in San Francisco Bay is the volume of freshwater discharge into the bay [*Peterson et al.,* 19891. Evidence for this control is that salinity in the bay has considerably more variability than that in the outside ocean. This contrast is illustrated by the annual range and the anomalous variability of the monthly mean salinity at Fort Point near the mouth and at the Farallon Islands, about 30 km offshore. Fort Point has an annual range of about 4.3 practical salinity units (psu) and maximum variability during spring with standard deviations exceeding 2 psu. Farallon Islands has an annual range of about 1.0 psu and a monthly standard deviation less than 1 psu. Most of the freshwater discharge, with an annual average of about 800 $m^3 s^{-1}$, flows from the western flanks of the high Sierra Nevada, through the estuary, to the eastern Pacific Ocean (Figure 1). The mediterraneanlike climate in this region has great seasonality, with highest freshwater flows in spring and lowest in early fall. Consequently, estuarine salinity is minimum in spring and maximum in fall. As a general rule, the annual amount of precipitation is the primary factor controlling mean monthly river flow and therefore the salinity variability in the estuary. The cool season precipitation influence propagates through the snowpack and water supplies in the mountains, the runoff from the watershed, and the conditions in the estuary.

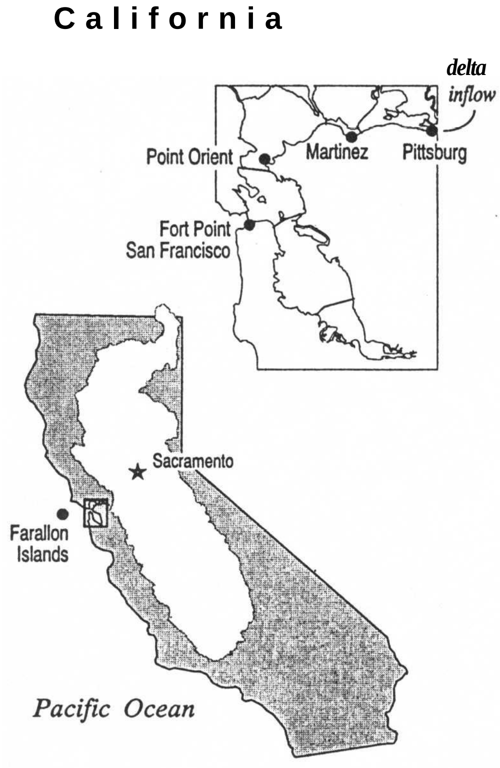

Fig. 1. San Francisco Bay, its drainage basin, and the adjacent coastal ocean.

Previous studies [e.g., Peterson et al., 1989] have demonstrated that winter precipitation has a strong influence on the salinity in the bay. Most of the variability in winter precipitation in the region can be attributed to large-scale anomalous atmospheric circulation patterns [Namias, 1978; *Klein and* Bloom, 19871. In this study we look further by considering how spring climate variability modulates the effects of wet versus dry winters. It is not a coincidence that the highest fall salinity peaks usually have been preceded by warmer than average springs (Figure 2). Anomalously warm and/or dry springs tend to produce earlier snowmelt, leading to a reduction of freshwater flow in summer and a higher peak salinity in the fall.

SEASONAL CLIMATE INFLUENCES

There are several processes that influence the salinity in San Francisco Bay, but the dominant factor is the amount of freshwater flow through the estuary. For example, in a linear model of monthly surface salinity (SS) anomalies at Fort Point over a long (1922–1986) record [Peterson et al., 1989], 86% of the variance of the observed SS anomaly was accounted for by a three-term linear combination of monthly anomalous discharge during the present and previous 2 months. Owing to the time lag between precipitation and flow, the seasonal climatic interpretation of this influence is not immediately clear. Winter has the greatest precipitation (approximately 55% of the mean precipitation occurs in December, January, and February) and also the greatest monthly anomaly variability in the watershed, so it is likely that winter precipitation is the strongest influence. However, spring climate variability also produces significant fluctuations in precipitation and temperature, and these would also perturb the freshwater flow through the delta and thus affect the bay salinity.

To better quantify the seasonal makeup of these influences, a multiple regression model of August–September SS was constructed on the basis of fall, winter, and spring precipitation and temperature. SS usually reaches its annual maximum during the August–September period. The salinity is from the 1922–1988 record from Fort Point at the mouth of San Francisco Bay, and the precipitation and temperature are National Climatic Data Center (NCDC) divisional averages of Sacramento and San Joaquin drainages, averaged together, for the same period. Winter is the average of December, January, and February, and spring is the average

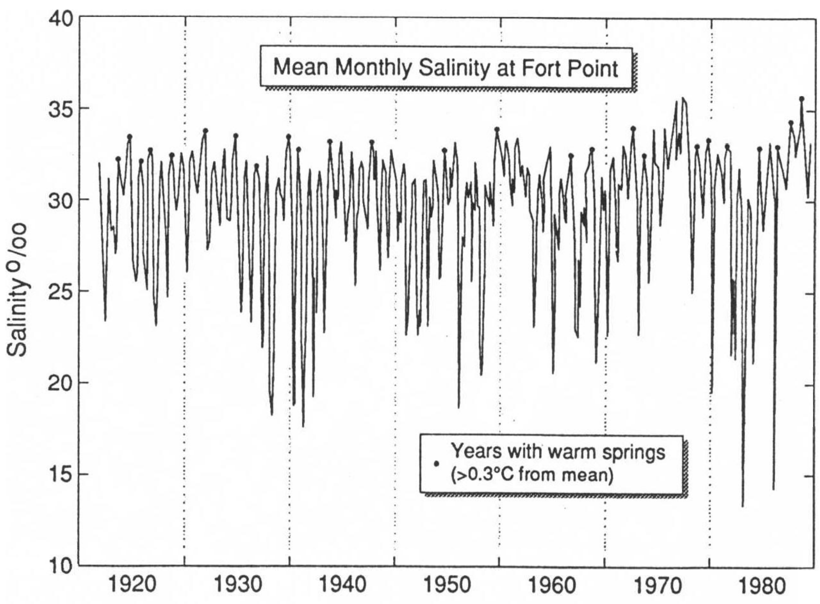

Fig. 2. Mean monthly salinity at Fort Point. The years with warm springs are based upon anomalies from the 1895 through 1986 mean from the Sacramento–San Joaquin divisional data.

of March, April, and May. This linear model accounts for 54% of the August–September SS variance, and four significant predictors emerge. It is important to note that this model consists of seasonally averaged inputs and is not designed to optimize the SS variance accounted for but rather to indicate the relative contributions of the predictors. The relative importance of the predictors is provided by the "beta" coefficients, the weights that would be attached to the predictors if they and the SS predictands were normalized by their standard deviations. Confirming the strong effect of winter precipitation, its beta coefficient was largest of all the predictors, with a value of –0.52. Of lesser magnitude, but still important, were spring precipitation and spring temperature, with beta coefficients of –0.21 and +0.21, respectively. The previous fall precipitation, which is strongly related to the initial salinity level at the beginning of the water year, is also a factor, with a beta coefficient of –0.23. Winter and fall temperature did not meet the 95% significance threshhold, while the four predictors noted above exceeded the 97.5% significance level. Winter precipitation is nearly uncorrelated with spring precipitation and spring temperature, and alone, it contributes about 36% of the August–September SS, so the two spring variables jointly contribute about 18% of the variability. Spring precipitation and temperature do not contribute entirely independently, as they are negatively correlated and to a greater extent than during any of the other seasons. Using the 51-year (1931–1991) record of seasonal averaged divisional temperature and precipitation at the NCDC Sacramento and San Joaquin divisions, the seasonal precipitation versus temperature correlations are ρ = 0.13, –0.55, –0.22, and –0.36 for winter, spring, summer, and fall, respectively.

Composites of extreme historical cases reveal that the development of high and low August and September Fort Point SS typically has nearly 1 year of buildup of persistent anomalous conditions. The composites, shown in Figure 3, indicate that these summer extremes often begin with high or low salinity at the beginning of the water year (October–September). The August and September SS is the average of the two monthly mean values and is abbreviated Augsep SS in the following discussion. Anomalies for the two cases were calculated by subtracting the 1922–1988 long-term monthly mean from the average of the monthly SS values for the 16 highest and lowest Augsep SS cases. The differences shown in Figure 3 are highly significant. From November of

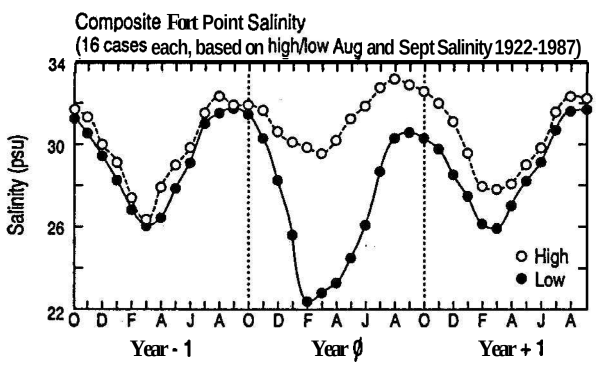

Fig. 3. Composite monthly salinity at Fort Point for a 3-year sequence: year – 1, year 0, and year +1, corresponding to high and low August and September salinity during year 0.

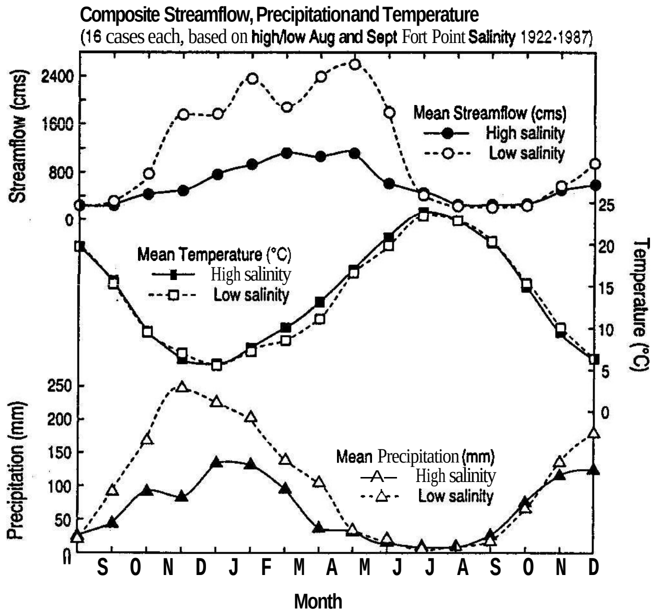

Fig. 4. Composite monthly streamflow, precipitation, and temperature in the San Francisco Bay region corresponding to high and low August and September salinity at Fort Point.

the previous calendar year to the high or low Augsep SS through December of the calendar year, the composite SS anomalies range from 0.5 to 1.2 standard deviations of each particular month's time series. These anomalies exceed the 95% confidence of being different from zero. Interestingly, even though the cases are chosen on the basis of extreme anomalies during Augsep, the greatest differences between the two cases are exhibited during January through June, with differences exceeding 5 psu. Also, once established, the anomaly tends to persist until the spring of the following year, albeit at a weaker amplitude.

The evolution of streamflow, precipitation, and temperature associated with high/low Fort Point Augsep SS anomalies is shown by the composites in Figure 4. As in the SS composite of Figure 3, 16 cases are included in each of the high and low SS composites. Corresponding to the high/low Augsep SS, streamflow is decidedly low/high from December through June. Over the water year the discharge for high Augsep SS cases averages 67% of its long-term annual mean and that for the low Augsep SS cases averages 146%. The difference in flow between the high and low scenarios is largest in May when seasonal flow is maximum. The may difference is about 1500 m^3 s^{-1}, nearly as large as the long-term mean flow in May (about 1700 m^3 s^{-1}).

In terms of local climate forcing, the composite flow anomalies are well related to the composite precipitation anomalies. Consistent with the streamflow, the high/low Augsep SS cases exhibit low/high precipitation for several of the antecedent months during fall, winter, and spring. Between October and April the composite precipitation anomalies range from 25 to over 50% of their long-term monthly mean and exceed the 95% confidence level of being different from zero, using a two-tailed t test.

The temperature "signal" is much more confined than that of precipitation. Significant temperature anomalies do not occur throughout the year but do occur during March and April. High Augsep SS is preceded by warmer than normal

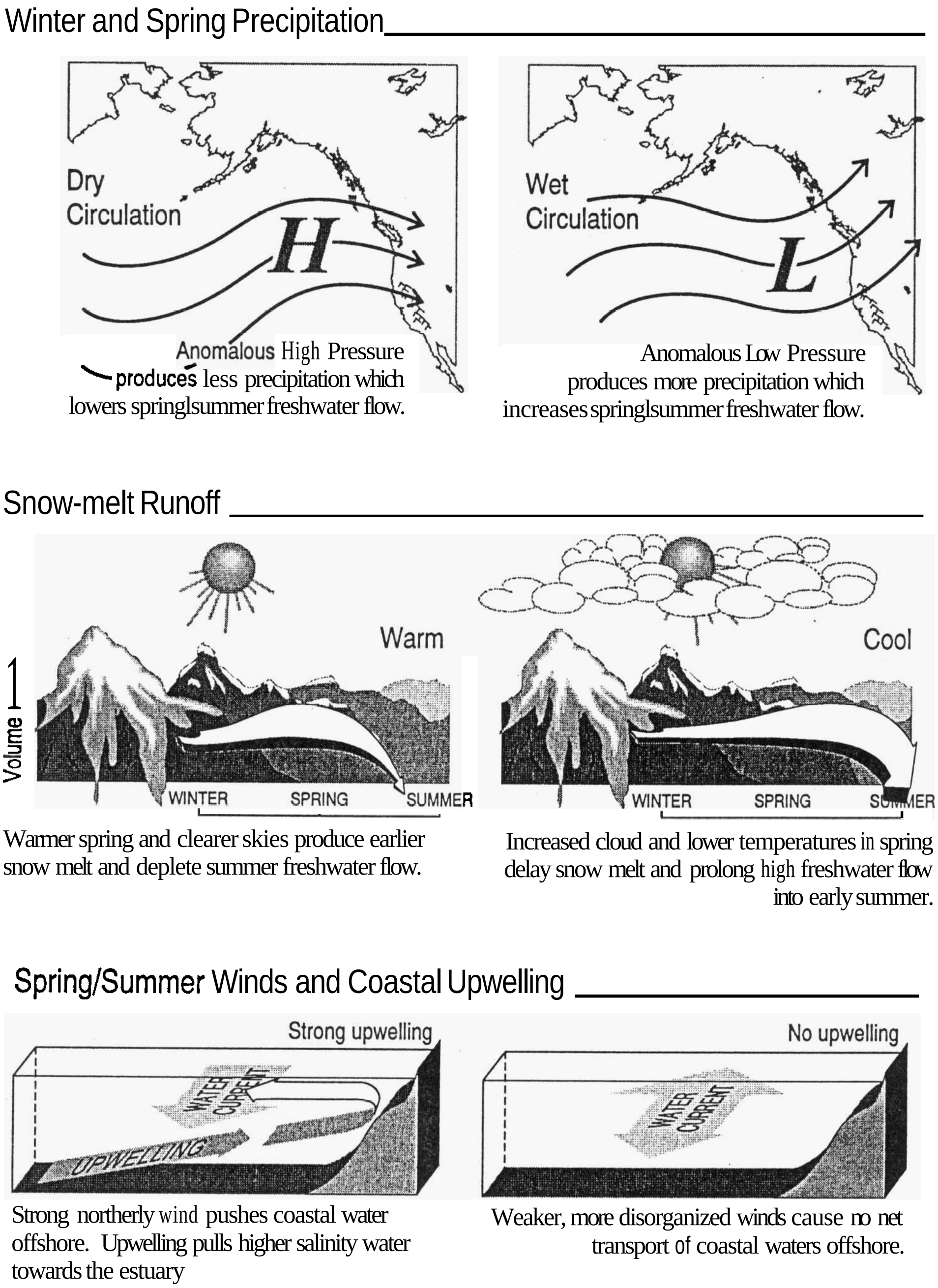

Fig. 5. Cartoon of physical processes affecting the surface salinity in the San Francisco Bay estuary.

spring temperatures, and low Augsep SS was preceded by cooler than normal temperatures. During March and April the temperature anomaly differences exceed 1.5°C, compared to their monthly standard deviations of 1.2" and 1.7°C; the differences between the anomalies in these two months exceed the 95% confidence level.

Each of the flow, precipitation, and temperature variables has significant anomalies preceding the high or low Augsep SS but not coincident with them. As shown in Figure 4, the precipitation signature appears as far back as October and November, and major anomalies occur during December through April. The temperature signal occurs later in spring when mean temperatures are close to the threshold where significant snowmelt runoff may be early or delayed. However, during the summer period there is little signal. During July through September (the period of the chosen high/low SS) the composite flow for the two extremes is virtually the same, indicating that the summer salinity in the bay is largely driven by prior variations in freshwater flow during winter and spring.

A general picture of the influences on San Francisco Bay SS is presented schematically in the upper two panels of the cartoon in Figure 5. The strongest impact (top panel) is the winter precipitation, which is driven by the atmospheric circulation in the North Pacific Ocean. The link between patterns of the winter atmospheric circulation over the North Pacific and subsequent streamflow in the Sierras and in other western streams is discussed by *Cayan and Peter-*

son [1989]. If winter precipitation is high, the runoff into the estuary during winter and subsequent months tends to be high, and SS in summer tends to be low. If winter precipitation is low, seasonal runoff tends to be low, and SS in summer tends to be high. The springtime climate influence, depicted in the middle panel, encompasses both the influence of temperature and precipitation. If spring precipitation is heavy, skies are cloudy and temperature is cool, so overall runoff is relatively high. Furthermore, the peak runoff is delayed into late spring and early summer because of the snowpack that persists in the Sierra Nevada. On the other hand, dry springs have clear skies, warm daytime temperatures due to stronger solar insulation, and, overall, a tendency toward less total runoff. Also, peak runoff during warm springs is earlier than that in cool springs [*Aguado et al.*, 1992]. Finally, a secondary influence upon the estuary that is considered later in the paper is that of the outside ocean, as portrayed in the bottom panel of Figure 5.

In the subsequent analyses our strategy is to begin with extreme categories of spring climate variations and examine their effects upon the bay salinity. There are three reasons why we have chosen to focus on the springtime effects. First, the evidence from the above observations indicates that spring climate variability has sufficient impact upon San Francisco Bay SS to merit an independent study. Winter climate influences upon the regional streamflow are discussed by *Cayan and Peterson* [1989], *Aguado et al.* [1992], and *Cayan et al.* [1993]. Their influence upon San Francisco Bay salinity, especially the link to atmospheric circulation, is discussed by *Peterson et al.* [1989]. Second, concerning future climate changes, this is an especially important season because the temperature threshhold for snowmelt-driven runoff occurs during spring in most mountain watersheds. In conjunction with peak runoff, the seasonal decline in heavy precipitation, and large summer imgation demands, much of the diversion of freshwater discharge from the upper end of the estuary and upstream watershed occurs during spring. Spring is the period when maximum freshwater diversions are extracted from the upstream watershed or the head of the estuary [*Peterson et al.*, 1989], and the freshwater spring flow volume is a major influence upon the fisheries or the San Francisco Bay riverine/estuarine system. Third, potential temperature changes that might arise fromglobal warming would presumably shift the runoff into the bay to an earlier peak. An analogy to this change might be the difference between years with cool springs and late runoff and years with warm springs and early runoff. Consequently, it is pertinent to study the effects of natural climate variability during this season of transition between the cool wet winter and the warm dry summer of the San Francisco Bay watershed.

The purpose of this paper is twofold. First, we will describe the influence of spring climate variability in determining the timing of freshwater spring flows and the resulting salinity variations in spring and summer in San Francisco Bay. Climate variables considered include precipitation, temperature, and atmospheric circulation patterns. Second, we investigate the estuarine response to forcing by the coastal ocean. It is seen that the oceanic influence is not as easily distinguished from the response to freshwater flows because it has a much smaller signal and because the ocean salinity field is forced by the same atmospheric circulation patterns as the estuary to produce oceanic salinity variations which are in the same direction as those driven by the associated anomalies of freshwater flow.

Air temperature might seem to be unimportant in determining the salinity level in the estuary, but it provides some direct as well as indirect bearing on the SS variability. Air temperature determines whether precipitation will occur as rain or snow and influences the timing of the spring melt. Moreover, we use the spring temperature in combination with precipitation to identify different atmospheric circulation patterns that affect the watershed, the estuary, and the outside ocean. Approximately 60 years of historical records demonstrate that cool and wet, warm and wet, cool and dry, and warm and dry categories are produced by quite distinct atmospheric circulation patterns and that these affect different responses in either the freshwater runoff or the salinity of the outside ocean.

DATA

Salinity observations were obtained from the U.S. Coast and Geodetic Survey (now the National Ocean Service) unpublished data for Fort Point and from Scripps Institution of Oceanography for the Farallon Islands. The primary measure of estuarine surface salinity used here is the monthly average of daily observations made near the Golden Gate bridge during water years 1922–1989. Measurements of surface salinity from the Farallon Islands (Figure 1) are from 1926–1986, with a large gap of missing data from 1943–1957. A water year is defined as the 12-month period October–September and is labeled by the calendar year of the January within that period. We use monthly averages to remove much of the variability caused by daily-fortnightly tidal effects. See *Peterson et al.* [1989] for more information on data.

The Fort Point monthly mean data are quite representative of the variability of salinity fluctuations throughout the estuary. Correlation coefficients for estuarine locations inside Fort Point toward the inside upper reaches of the estuary are as follows: Alameda (0.90), Point Orient (0.92), Martinez (0.86), Port Chicago (0.83), Pittsburgh (0.63), and Antioch (0.55). These values are correlations of the log of the SS anomalies (annual cycle removed) at these sites versus the SS anomalies at Fort Point. These correlations are highly significant (little chance of the true correlation being zero), as they are constructed from at least 23 and as many as 48 years of monthly data pairs for each site.

Streamflow into San Francisco Bay during the water years 1922–1989 is given by the estimated "delta flow," which is the combined flow of the Sacramento–San Joaquin River basins into the estuary. Streamflow data are provided by the California Department of Water Resources (1922–1930, from M. Roos, unpublished manuscript, 1971; 1930–1986, from S. Greene, unpublished manuscript, 1988). Accuracy of delta flows are believed to be in the range of 5 to 10%, although these percent errors are likely to be higher during periods of low summer flow (M. Roos, personal communication, 1991).

The air temperature and precipitation data used here are the mean divisional (average of several stations within areas) temperature and precipitation of the Sacramento and San Joaquin drainage regions. The divisional data, routinely calculated by the U.S. National Climate Data Center, are used because regions of anomalous temperature and precipitation tend to have broad spatial scales [*Karl and Knight*,

TABLE 1. The Eight Years Used in Each of the Four Spring Composites and Their Corresponding Spring Precipitation and Air Temperature Anomalies From the Average Value of the Entire Sacramento and San Joaquin River Basin Division

Climate Scenario	Year	Precipitation, mm	Temperature, °C
Cool and wet	1983	218	−1.1
	1948	174	−2.4
	1958	160	−0.4
	1982	145	−0.8
	1967	143	−2.1
	1963	125	−1.5
	1938	122	−0.9
	1935	108	−1.3
Warm and wet	1978	114	0.3
	1925	55	0.8
	1928	44	1.4
	1943	39	0.6
	1986	24	1.0
	1949	21	0.1
	1954	16	0.6
	1940	3	1.3
Cool and dry	1976	−108	−0.3
	1970	−96	−0.1
	1977	−84	−1.1
	1985	−73	−0.1
	1964	−71	−1.1
	1956	−70	−0.2
	1962	−68	−0.5
	1955	−65	−1.2
Warm and dry	1966	−131	1.7
	1934	−129	3.1
	1959	−127	1.3
	1972	−108	1.2
	1924	−88	1.5
	1968	−86	0.4
	1931	−85	2.1
	1984	−85	0.9

19851, especially during cool season months. Seasonal anomalies are from the 1895–1986 seasonal long-term average. It is noted that before 1931 the divisional data were not reported, so it was estimated at NCDC *[Karl and Knight, 1985]* from statewide average values of nearby states within the region via multiple regression.

Atmospheric circulation is inferred from monthly mean sea level pressure (SLP) gridded onto 5° latitude-longitude squares from the U.S. National Meteorological Center and the National Center for Atmospheric Research. This data set covers the period 1899 to the present *[Trenberth and Paolino,* 19801.

Coastal sea level height (SLH) has been measured by tide gages at the Presidio (near the Golden Gate bridge) from 1897 to the present *[Disney and Overshiner, 1925]* by the National Oceanographic and Atmospheric Agency (monthly average). An overall linear trend was subtracted from this time series to remove low-frequency variations caused, for example, by geological processes. Monthly sea level was adjusted by the regional sea level pressure at a factor of 0.01 m hPa^{-1} (1 cm $mbar^{-1}$) to correct for the local inverse barometric effect.

Several of these variables are seasonally averaged, where winter is December, January, and February; spring is March, April, and May, and so on.

SURFACE WEATHER AND ATMOSPHERIC CIRCULATION

To examine the influence of anomalous atmospheric circulation patterns on spring surface climate in this region, the years are divided according to spring precipitation and then further stratified into "warm" and "cool" groups. These categories are determined from Sacramento plus San Joaquin average divisional spring precipitation and temperature anomalies. The four categories (cool and wet, warm and wet, cool and dry, and warm and dry) are denoted CW, WW, CD, and WD, respectively (Table 1). In the following discussion, composite anomalies are determined for the eight wettest cool springs, eight wettest warm springs, eight driest cool springs, and eight driest warm springs from the divisional data since 1922. The precipitation and temperature anomalies averaged over the two divisions for these four 8-case composites were 149 mm and −1.3°C, 40 mm and 0.8°C, −79 mm and −0.6°C, and −105 mm and 1.5°C, respectively.

Considering the spatial structure of anomalies of spring average temperature and precipitation over an area covering the United States and western Canada, composites for the four categories indicate that the California anomalies are coherent, with like-sign anomalies that extend well beyond the state and with opposite-sign teleconnections that occur downstream and sometimes to the north. When expressed in terms of anomalies from their overall long-term mean spring values, the classification of spring precipitation and temperature into CW, WW, CD, and WD cases indicates that the WD and CW predominate over the WW and CD categories.

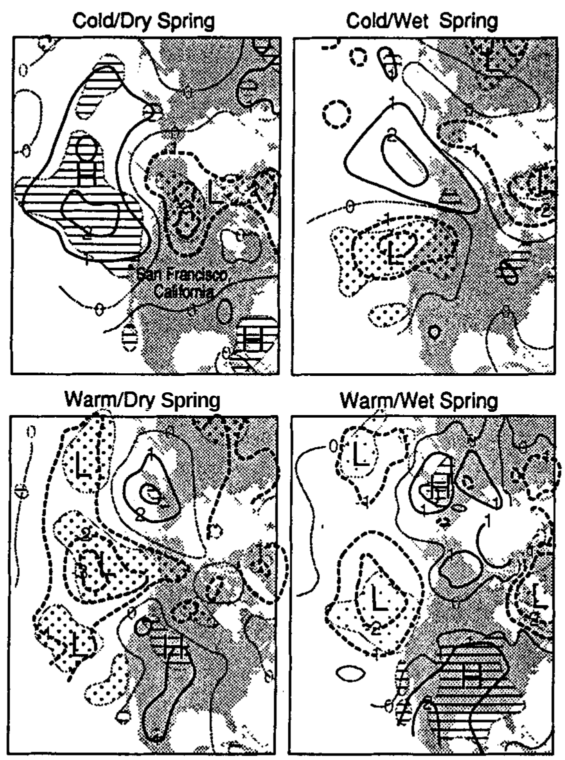

Fig. 6. Composite SLP anomalies (hectopascals) for CW, WW, CD, and WD springs (March, April, and May) from 1921–1986. Eight cases are included in each composited average. Shading (hatching for positive anomalies, stippling for negative anomalies) indicates anomalies significantly different from zero at the 90% confidence level via a t test.

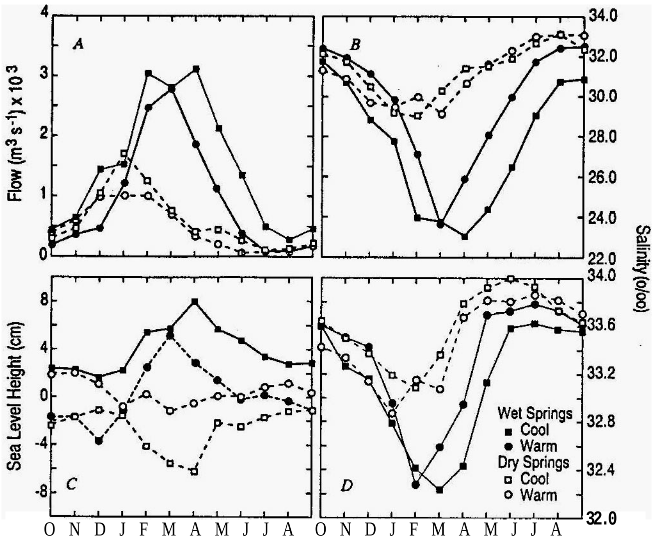

Fig. 7. (*a*) Composite delta flow, (*b*) estuarine SS, (*c*) coastal ocean sea level height, and (*d*) coastal ocean SS for CW, WW, CD, and WD springs as per Figure 6. Farallon Islands' SS in Figure 7d was not available for all 8 years in the composite average. Years included for each category were CW 1983, 1958, 1982, 1967, 1963, 1938, and 1935; WW 1978, 1928, 1986, and 1940; CD 1976, 1970, 1977, 1985, 1964, and 1962; WD 1966, 1934, 1959, 1972, 1968, 1931, and 1984.

The correlation between spring precipitation and spring temperature (divisional average data) is –0.55. That is, dry springs tend to be warmer (less clouds and greater solar insolation) and wet springs tend to be cooler (more clouds and advection of cooler air). Nonetheless, the WW and CD spring categories occur frequently enough to define a composite category with distinct physical characteristics. Although the years entering each composite are based on temperature and precipitation in California, they are also consistent with anomalies of spring snowpack (not shown) and streamflow (below) over much of the western United States.

Composite SLP anomalies for the four categories show that each category is associated with a distinct atmospheric circulation anomaly pattern (Figure 6). In both the CW and WW composites there is a prominent negative SLP anomaly centered to the northwest of California. The CW negative anomaly region is confined to the region east of about 150°W, with a positive anomaly center to the west centered at approximately 50°N, 165°W. The CW circulation produces a high-amplitude ridge and trough system across the North Pacific, with cool air advected southward on the east side of the high-pressure anomaly into the eastern North Pacific and the west coast. This circulation often produces "cutoff lows," which are low- to middle-latitude cyclonic features detached from the upper level westerly flow to the north. For WW springs the negative SLP anomaly region is more extensive, occupying most of the eastern North Pacific basin. Positive anomalies are located far to the northwest over Kamchatka and downstream over the central plains of the United States. The broad negative anomaly in the WW case is symptomatic of southward displaced westerly winds, vigorous storms, and a warm moist air mass injected into California from the eastern half of the North Pacific.

The cool versus warm classification also provides a sharper view of dry spring atmospheric conditions in California. In comparing the typical circulation patterns for the CD and WD categories they are markedly different even though both are dominated by a high pressure near California. The CD pattern has a broad region of positive SLP anomalies (high pressure) centered offshore at about 40°N, 150°W, with negative anomalies over Alaska and northern Canada that extend southward over the Rocky Mountains. This CD pattern drives cold air southward from the Gulf of Alaska and the interior of North America and produces cool temperatures throughout the western United States. In contrast, the WD pattern features positive SLP anomalies centered over Oregon and extending just offshore to the northwest, with negative anomalies in the eastern North Pacific north of Hawaii. This circulation inhibits cold Canadian air from penetrating southward and induces anomalous southerly flow into California, so that it and most of the West is warm. While the negative SLP anomalies signify active storms in the central North Pacific during WD cases, this circulation pushes them northward toward coastal Alaska.

River Basin and Estuarine Response

CW, WW, CD, and WD atmospheric circulation patterns produce characteristic river flows and estuarine salinity responses (Figures 7*a* and 7b). Corresponding significance levels are provided in Table 2. During wet and dry regimes, delta flow persists relatively longer in cool than in warm springs. For both the wet and dry pairs the estuarine response is to have lower salinity during summer and fall for cool springs relative to warm ones, although the dry, or low-flow, reposes are less distinct than those for the wet pair (Figure 7*b*).

During the WW regime, delta flow peaks in March and rapidly declines to its minimum in July–August. Corresponding WW salinity is lowest in March and thereafter increases to its maximum in August–September. In contrast, the CW flow peak is delayed by the later snowmelt until April, and flow in successive months is considerably higher than WW until the late summer minimum in August. Such delays are evident in daily observations as well as in the monthly data [*Cayan*, 1991]. The CW salinity mirrors the peak and generally higher spring flow, with an April minimum and decidedly lower salinity throughout the remainder of the water year. Differences between CW and WW flow and salinity are highly significant, as judged by a two-tailed t test, and all differences from May through September exceed the 90% level of confidence (Table 2). It should be noted that the winter months preceding the eight CW spring cases had greater precipitation than did those preceding the WW springs. (The winters preceding CW springs had 26 mm more precipitation than winters preceding the WW springs and 50 mm (113%) more precipitation than the winter long-term mean. In comparison, CW springs had 149 mm (177%) more precipitation than the spring long-term mean.) This prior winter condition contributes to the higher flow and lower salinity during spring and summer of the CW versus the WW composites.

Among the four atmospheric scenarios, the largest difference in the salinity response is between CW springs and WD springs, with the difference in salinity as much as 3 psu during the late summer/early fall period (see Figure 7*b*). The schematic in Figure 8 is given to better visualize the physical

TABLE 2. The t Test Values for Differences Between Each Category for Delta Flow, SS, and SLH

		Month											
Variable	Category	Oct.	Nov.	Dec.	Jan.	Feb.	March	April	May	June	July	Aug.	Sept.
San Francisco Bay SS	CD-WD	1.1	1.0	0.5	0.2	−0.6	0.8	0.9	−0.1	−0.4	−0.4	0.0	−1.5
	CD-CW	0.6	1.7	1.9*	0.7	2.3*	2.5*	6.9†	6.4†	4.2*	3.9†	3.4†	2.7*
	CD-WW	0.4	−0.3	−1.0	−0.4	1.1	3.1†	3.5†	3.0*	1.7	1.2	1.1	0.4
	WD-CW	−0.5	0.5	0.7	1.0	3.8†	2.3*	7.4†	9.9†	6.1†	6.3†	6.5†	4.7†
	WD-WW	−1.8*	−1.2	−1.1	−0.2	2.9*	3.0†	3.4†	4.1†	3.3†	3.0†	2.2	2.1
	CW-ww	−1.1	−1.9*	−3.0*	−1.5	−1.7	0.1	−1.7	−3.5†	−3.1†	−4.0†	−4.8†	−3.9†
Delta flow	CD-WD	−0.9	−0.5	0.1	0.8	0.5	0.2	0.6	1.3	1.7	1.1	0.9	0.5
	CD-CW	−0.8	−1.4	−0.8	0.2	−2.1*	−2.2*	−7.5†	−5.5†	−4.3†	−2.5*	−2.0	−1.9*
	CD-WW	1.5	1.0	1.4	0.5	−1.6	−3.7†	−4.6†	−2.4*	−3.0	1.0	1.7	0.4
	WD-CW	−0.2	−0.2	−0.7	−1.2	−2.8	−2.3*	−8.2†	−0.3*	−5.7†	−2.8*	−2.0*	−2.2*
	WD-WW	2.1*	1.0	3.0	−0.4	−2.3*	−4.2†	−5.3†	−6.0†	−3.7†	−0.5	0.2	−0.2
	CW-WW	1.6	2.4*	2.6*	0.7	0.6	0.0	2.8†	4.0†	4.0†	2.7*	2.4*	2.2*
Sam Francisco SLH	CD-WD	−1.7	−1.4	−0.7	−0.2	−1.8*	−1.7	−2.8*	−1.2	−2.2	1.3	−1.3	−0.9
	CD-CW	−1.9*	−1.2	−1.0	−1.3	−2.4*	−2.9*	−6.6†	−3.8†	−5.0†	−2.3*	−1.9*	−1.5
	CD-WW	−0.4	0.0	1.2	−0.1	−2.7*	−4.2†	−5.1†	−1.9*	−1.3	−1.0	−0.7	0.0
	WD-CW	0.2	0.1	−0.2	−1.1	−1.4	−2.0*	−4.9†	−3.4†	−3.9†	−1.5	−0.8	−0.9
	WD-WW	1.6	1.5	1.8*	0.1	−1.2	−3.5†	−2.8*	−3.0	0.1	0.7	1.0	0.8
	CW-WW	1.8*	1.2	2.4*	1.2	0.8	0.2	3.4†	5.3†	2.7*	1.9*	1.7	1.5

SS, surface salinity; SLH, sea level height. CD, cool and dry; WD, warm and dry; CW, cool and wet; and WW, warm and wet.
*Values exceeding the **90%** two-tailed *t* test significant threshold of **±1.76.**
†**Values** exceeding the **99%** threshold of **22.98.**

processes affecting the estuary. This depicts the influences upon the Bay: its upstream watershed, the outside ocean, and to some extent, direct effects of the atmosphere overhead. The unifying agent that organizes each of these processes is the atmospheric circulation. On the monthly time scales considered here, estuarine variability, salinity in this instance, is linked back to anomalous atmospheric circulation through precipitation and runoff from the upland river basin (steps 1 and 2 in Figure 8). In fact, most of the variability in salinity near the mouth of the San Francisco Bay correlates with delta flow (ρ^2 = 0.86). While this leaves only a small fraction of variability unaccounted for, there is marked variability along the outside coastal ocean [*Roden*, 1961; Huyer, **1984]**, and it is important to identify its influence.

COASTAL OCEAN RESPONSE

One might be tempted to overlook the influence of the coastal ocean on San Francisco Bay because variations in river discharge are the dominant influence upon properties in the Bay. The coastal ocean and possibly the estuary itself (not explored here) responds to the same atmospheric forcing pattern as the river basin (as noted in steps 4 and 5 in Figure 8). Strengthened northerly (equatorward) winds along the coast during CD and strengthened southerly (poleward) winds during CW can be inferred from the anomalous SLP field (geostrophic wind) in Figure 6. These anomalies imply greater offshore (CD) or onshore (CW) Ekman transport from the wind-driven circulation [Pares-Sierra and O'Brien, 19891. Extreme negative SLH anomalies occur in response to CD spring atmospheric patterns; extreme positive SLH anomalies occur in response to CW and to some extent WW spring atmospheric patterns (Figure 7*c*). Note that the high persistent CW SLH anomalies also include 1958 and 1983, years with a strong remote tropical influence [Pares-Sierra and *O'Brien*, 19891. Positive differences between CW and CD SLH and Fort Point SS exceed the 95% confidence level over the February–July period, with particularly large values in March and April (not shown). These CW and CD coastal SLH differences are supported by a more limited set of offshore surface salinity from the Farallon Islands. Again, CW and CD composites are the most different (Figure 7d). The intermediate SLH anomaly and Farallon surface salinity values associated with the scenario suggest atmospheric circulation that is less favorable for offshore-onshore responses during WD regimes.

Time series models indicate that this low-SS (CW) and high-SS (CD) effect near the mouth of the estuary is of much lower importance than "flushing" by discharge through the delta, however (see Peterson et al. **[1989]** and comments below). For example, monthly mean coastal ocean SS anomalies at the Farallon Islands are typically ±0.5 psu. Steady state response of SS near the mouth of the estuary (Fort Point) is estimated to be 3.2 psu per 1000 $m^3\ s^{-1}$ of delta flow. Thus a coastal ocean change of 0.5 psu is equivalent to a change in delta flow of about 150 $m^3\ s^{-1}$ or about 20% of the mean annual flow. Another limitation on the effect of upwelling on the estuarine salinity is the maximum salinity at depth in the vicinity of the offshore continental shelf break. This value is about 34.2 psu near the Farallon Islands [*Conomos* et al., **1979]**. While this value is significantly

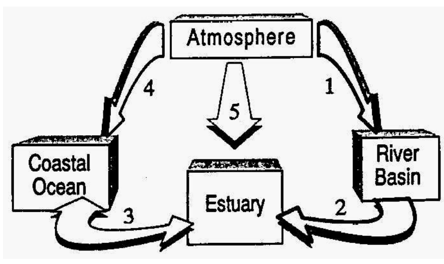

Fig. **8.** Schematic of linkages between atmosphere, watershed, coastal ocean, and estuary. Strongest linkages are indicated by darkest arrows.

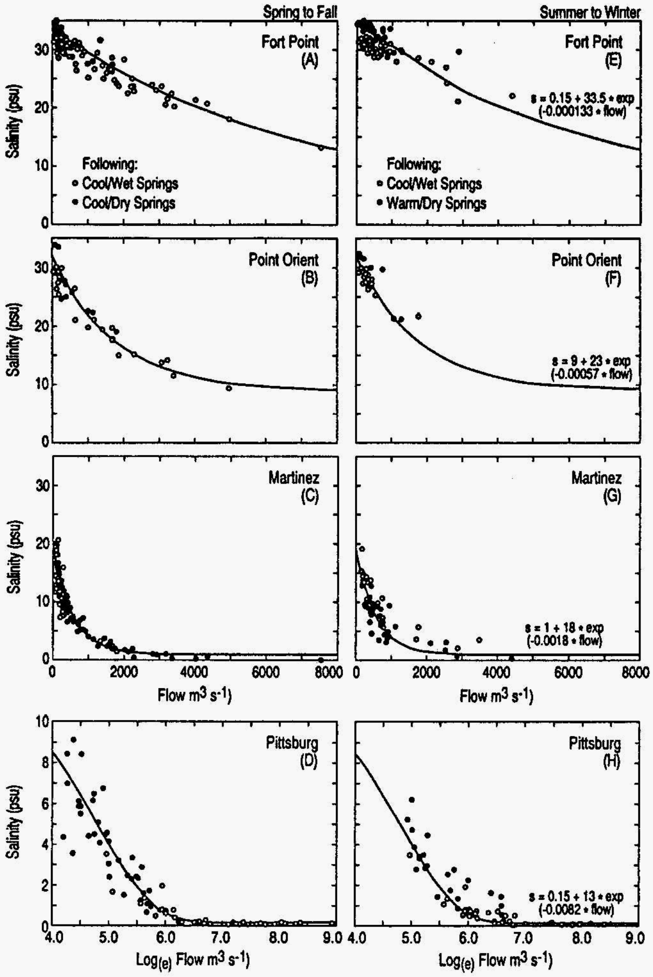

Fig. 9. SS and delta flow at four different sites, from Fort Point at the mouth to Pittsburg near the interior Sacramento–San Joaquin delta. The exponential equation shown on the panels is an approximation from all the data to provide a line of reference. (*a*)–(*d*) Declining delta flow from spring to fall, corresponding to CW and CD springs. Note the tendency of CD salinities to be higher than CW for higher flows at Fort Point and Point Orient but not at Martinez and Pittsburg. (*e*)–(*h*) Scenarios of rising summer to winter delta flow following CW and WD springs. Note the tendency of WD salinities to be higher than CW salinities for higher flows at Pittsburg and Martinez but not at Point Orient and Fort Point.

above the maximum long-term monthly mean SS value at Fort Point during August and September, it is less than monthly extreme values exceeding 35 psu that have occurred within the historical record. Thus other processes must also contribute to elevated salinity in the estuary.

Much of the ocean influence must be carried out by the action of the wind. Comparing the four cases, the difference in the ocean mean surface wind near the California coast was greatest between the CD and the CW cases. This is especially true for the southerly (south-to-north) wind component in the CD-CW difference. From surface weather reports collected in the Comprehensive Ocean Atmosphere Data Set (COADS) [*Woodruff et al.*, 1987; *Cayan*, 1992], the region (27°–33°N, 117°–133°W) offshore from California has an area-average difference in the southerly wind of about 1.1 m s^{-1}, the CW case having a stronger southerly wind than the CD. This difference can be inferred from the composite sea level pressure maps in Figure 6. As also can be inferred, the other cases exhibit significant anomalies and case-to-case differences in wind strength, but the regions these appear in are remote (not strong along the California coast like the CD-CW difference).

To conclude the analysis of oceanic and freshwater influences, we compare the relation between SS and freshwater flow at different locations in the estuary. Over the annual cycle, peak flows in spring (March–May) produce the lowest salinities in the estuary. As this flow recedes during late spring and summer, high salinities return, reaching a maximum value in late summer or early fall. This maximum salinity level depends on the history of river flow: it is highest after long periods of low flow and lowest after long periods of high flow. Spring temperature provides the mechanism to modulate this timing by hastening the runoff in warm springs and delaying it during cool springs. In that spring is the period of maximum freshwater diversion from the estuary, human activity tends to mimic a warm spring scenario.

A contrast between the oceanic versus the freshwater influences is provided by tracing the SS variability at different sites through the estuary. Figure 9 illustrates the relationship between salinity and flow at four different sites, from Fort Point at the mouth to Pittsburg near the interior Sacramento–San Joaquin Delta. Two climate effects altering the SS flow characteristics are identified. We isolate two pairs of subsets of the data: (1) the CD and CW cases which have maximum and minimum salinity composite values in the outside ocean (Farallon Islands) and (2) the WD and CW cases which have maximum and minimum salinity composite values in the interior of the estuary (Pittsburg and Martinez).

First is an apparent affect of variable salinity in the coastal ocean. On the basis of the Farallon Islands SS, coastal ocean salinity is high in CD springs and low in CW springs. Reasons for this difference, which is greater between CD and CW springs than any of the other pairs of cases, appear to stem from the coastal winds which have the strongest northerly component during the CD atmospheric pattern and the strongest southerly component during the CW atmospheric pattern (Figure 6 and COADS surface wind calculation). Thus near the mouth of the Bay the SS flow relation tends to show slightly higher SS values per unit flow in CD than in CW years. This is illustrated by the Fort Point SS flow plots of all CD versus all CW spring, summer, and fall months in Figure 9*a*, and as an average over the annual cycle for the two cases in Figure 10. As expected, this effect appears to fade as we procede inland into the estuary, as seen in limited observations at Point Orient (Figure 9*b*). The effect is not present at stations farther inland, represented by Martinez or Pittsburg (Figures 9*c* and 9*d*) because the relative proportion of seawater becomes more and more diluted. Because of the effect of the cumulative flow during several preceding months, the salinity/flow relation varies over the annual cycle, as can be seen in Figure 10. Figures 9*a*–9*d* indicate the salinity response when flow is declining during spring to fall. The solid circles represent periods during which the ocean may have increased the Bay SS. These solid circles are CD cases when coastal upwelling is (or has been) probably more intense and tend to be higher salinities than the open circles which represent CW cases and lack of coastal upwelling.

In contrast to the ocean influence, the second effect on San Francisco Bay salinity is due to flushing by freshwater

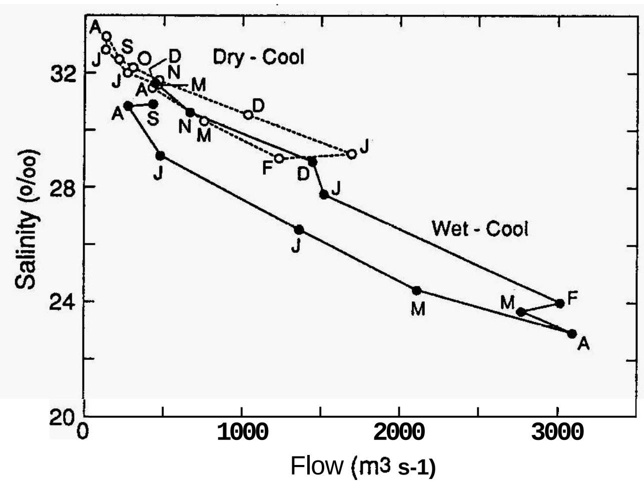

Fig. 10. Estuarine salinity–delta flow relationship for CD spring composite and CW spring composite at Fort Point. Composites based on 8 years for each case.

discharge. This influence acts throughout the history of an annual cycle, as the removal of salt by fresh water is cumulative, but it has different signatures on different parts of the estuary. Near the mouth of the estuary this influence is most important in late winter, and near the head of the estuary it is most important in late summer and fall. Figures *9e–9h* indicate the rising flow period between fall and winter, so this represents the "recovery" of the estuary from high (solid circles) or low (open circles) summer SS of the WD or CW cases, respectively. Thus the SS flow relation near the head tends to show the greatest difference in SS per unit flow in summers and falls following WD springs versus summers and falls following CW springs. This is exemplified by Pittsburg and Martinez in Figures *9g* and *9h*. In contrast, there is not nearly as strong an effect near the mouth of the estuary, as shown in Figures *9f* and *9e* by Point Orient and Fort Point.

SUMMARY AND IMPLICATIONS

Two processes that force surface salinity (SS) in the San Francisco Bay Estuary are freshwater river flow (a large effect) and variability in coastal ocean salinity (a small effect). The strongest impact from the freshwater flow is its magnitude, but there is a second, more subtle effect from the timing of flow. There is a very clear response of SS to the discharge through the Sacramento River/San Joaquin River Delta. In turn, the discharge is driven by regional precipitation and temperature conditions, which are regional climate variations that are driven by atmospheric circulation patterns over the eastern North Pacific and western North America.

The focus of this study is upon the effects of regional climate variations during spring rather than those during winter. As demonstrated by modeling [*Peterson et al.*, 1989], winter precipitation and monthly flow in the delta have a strong control on the overall salinity variation in the estuary during the water year. But it is also clear that spring temperature and precipitation, together, modify SS in the estuary by affecting the timing and to some extent the magnitude of spring flow. For example, warm dry (WD) springs tend to produce the highest salinity in the summer in San Francisco Bay (especially in the interior of the estuary), while cool wet (CW) springs tend to produce the lowest salinity in summer.

Springtime conditions in the coastal ocean (such as in Figures *7c* and *7d*) also appear to modify the salinity response to delta flow, especially for cool dry (CD) versus CW springs (Figure *10*). Equatonvard winds prevail during CD. This causes offshore Ekman flux. which lowers sea level and causes coastal upwelling, resulting in higher salinity. During the CW regime, sea level is high and sea surface salinity is low, and the two forcing factors, river flow (lowers salinity) and coastal ocean (a lower salinity), are additive. Conversely, during the CD regime the coastal ocean sea surface salinity is high, and the two factors are opposed or tend to cancel. It should also be noted that the salinity flow responses to coastal ocean conditions associated with the two warm regimes are intermediate between these two extremes (not shown). This intermediate response of the estuary appears consistent with the observed intermediate SLH and Farallon Islands salinities which also show intermediate anomalies relative to the cool regimes. Step 4 (Figure 8), the link between atmospheric forcing and coastal ocean salinity seems clear: equatorward winds result in coastal upwelling, which brings saltier water to the surface. However, because observations from the coastal ocean are sparse in both time and space, the mechanism of the outside ocean influence on San Francisco Bay is not known.

Intuitively, the effect of coastal ocean variability must decrease with increasing distance inland, and the effect of delta flow on sea surface salinity must decrease with increasing distance seaward from the delta. Evidence from landward stations indicate that interior estuarine salinity is controlled more strongly by delta flow and less by fluctuations in the coastal ocean (such a distinction in the salinity flow pattern, as in Figure 9, appears to fade with distance inland for available observations noted in the section on data above). Our understanding of the coastal ocean behavior is not clear, as measurements are scarce. However, some of the SLP, river flow, SLH, and SS linkages reported here have been observed on daily and weekly time scales [*Walters and Gartner*, 1985].

The framework provided here should assist in the difficult topic of sorting out human from natural-caused variability, for example, to address the general issue of the effect of reductions in freshwater flows and, in particular, the springtime variability of properties in the San Francisco Bay estuary. For example, the effects of spring climate variations on spring–summer delta flow would modulate any further artificial reductions in spring delta flows, accentuating the salinity increase in warm springs and counteracting them in cool springs.

Finally, what if hypothesized global climate warming drives this system toward the warm (wet or dry) categories? Previous studies by *Gleick* [1987], *Roos* [1989], *Lettenmaier and Gan* [1990], and *Aguado et al.* [1992] indicate that regional climate warming (by 1° to 4°C) would produce a marked change toward earlier peak spring runoff. The behavior during the historical record examined here suggests that if other factors remained the same, earlier peak flows would produce higher summer and fall salinity in San Francisco Bay, since the freshwater influence in late spring in summer would be diminished. Such a change might affect the

use of the upper estuary water for agricultural and human consumption because higher artificial discharges of fresh water into the estuary would be required to reduce the late summer and fall salinity to present levels.

Acknowledgments. Cayan was supported by the USGS via an Intergovernmental Personnel Agreement, by the University of California Water Resources Center, project UCAL-W-720, and by the NOAA Climate Program Office through the Experimental Climate Forecast Center. Thanks to L. Riddle for calculations and graphics, M. Schultz and especially J. DiLeo-Stevens for illustrations, and L. Thomas for typing the manuscript. Excellent reviews were provided by S. G. Monismith, F. H. Nichols, M. A. Noble, L. K. Rosenfeld, R. A. Walters, D. Lettenmaier, and an anonymous reviewer.

REFERENCES

Aguado, E., D. R. Cayan, and L. G. Riddle, Climate fluctuations and the timing of West Coast streamflow, *J. Clim.*, in press, 1992.

California State Water Resources Control Board, Water quality control plan for salinity, San Francisco Bay/Sacramento–San Joaquin Delta Estuary, *Rep. 91-15*, 16, 17, *WR*, Sacramento, 1991.

Carlton, J. T., J. K. Thompson, L. E. Schemel, and F. H. Nichols, Remarkable invasion of San Francisco Bay (California, USA) by the Asian clam *Potamocorbula amurensis*, I, Introduction and dispersal, *Mar. Ecol. Prog. Ser.*, 66, 81–94, 1990.

Cayan, D. R., "Cool" vs. "warm" winter precipitation and its effect on streamflow in California, in Proceedings of the 7th Annual Pacific Climate (PACLIM) Workshop, edited by J. Betancourt and V. Thorp, *Tech. Rep.* 26, pp. 91–100, Calif. Dep. of Water Resour. Estuarine Ecol. Study Program, Sacramento, 1991.

Cayan, D. R., Variability of latent and sensible heat fluxes estimated using bulk formulae, *Atmos. Ocean*, 30, 1-42, 1992.

Cayan, D. R., and D. H. Peterson, The influence of North Pacific atmospheric circulation on stream flow in the west, in *Aspects of Climate Variability in the Pacific and the Western Americas, Geophys. Monogr. Ser.*, vol. 55, edited by D. Peterson, pp. 375–397, AGU, Washington D. C., 1989.

Cayan, D. R., L. G. Riddle, and E. Aguado, The influence of precipitation and temperature on seasonal streamflow in California, *Water Resour. Res.*, in press, 1993.

Cloern, J. E., Does the benthos control phytoplankton biomass in South San Francisco Bay (USA)?, *Mar. Ecol. Prog. Ser.*, 9, 191–202, 1982.

Cloern, J. E., and F. H. Nichols (Eds.), *Temporal Dynamics of an Estuary: San Francisco Bay*, 237 pp.. Junk, Dordrecht, Netherlands, 1985.

Conomos, T. J. (Ed.), *San Francisco Bay: The Urbanized Estuary*, 493 pp., American Association for the Advancement of Science, Washington, D. C., 1979.

Conomos, T. J., R. E. Smith, D. H. Peterson, S. W. Hager, and L. E. Schimmel, Processes affecting seasonal distributions of water properties in the San Francisco Bay estuarine system, in *San Francisco Bay: The Urbanized Estuary*, edited by T. J. Conomos, pp. 115–142, American Association for the Advancement of Science, Washington, D. C., 1979.

Disney, L. P., and W. H. Overshiner, Tides and currents in San Francisco Bay, *Spec. Publ.* 115,125 pp., U.S. Coast and Geodetic Surv., U.S. Dep. of Commer., Washington, D. C., 1925.

Gleick, P. H., The development and testing of a water balance model for climate impact assessment: Modeling the Sacramento basin, *Water Resour. Res.*, 23, 1049–1061, 1987.

Huyer, A., Hydrographic observations along the CODE central line off Northern California, 1981, *J. Phys. Oceanogr.*, *14*, 1647–1658, 1984.

Karl, T. R., and R. W. Knight, Atlas of monthly and seasonal precipitation departures from normal (1895–1985) for the contiguous United States, *Hist. Climatol. Ser. 3–12*, 213 pp., Natl. Clim. Data Center, Asheville, N. C., 1985.

Klein, W. H., and H. J. Bloom, Specification of monthly precipitation over the United States from the surrounding 700 mb height field, *Mon. Weather Rev.*, 115, 2118–2132, 1987.

Lettenmaier, D. P., and T. Y. Gan, Hydrologic sensitivities of the Sacramento–San Joaquin River basin, California, to global warming, *Water Resour. Res.*, 26, 69-86, 1990.

Namias, J., Multiple causes of the North American abnormal winter 1976–77, *Mon. Weather Rev.*, 106, 279–295, 1978.

Nichols, F. H., Increased benthic grazing: An alternative explanation for low phytoplankton biomass in northern San Francisco Bay during 1976–1977 drought, *Estuarine Coastal Shelf Sci.*, 21, 379–388, 1985.

Nichols, F. H., J. E. Cloern, S. N. Luoma, and D. H. Peterson, The modification of an estuary, *Science*, 31, 567–573, 1986.

Pares-Sierra, A., and J. J. O'Brien, The seasonal and interannual variability of the California current system: A numerical model, *J. Geophys. Res.*, *94*, 3159–3180, 1989.

Peterson, D. H., et al., Climate variability in an estuary: Effects of river flow on San Francisco Bay, in *Aspects of Climate Variability in the Pacific and the Western Americas, Geophys. Monogr. Ser.*, vol. 55, edited by D. H. Peterson, pp. 419-442, AGU, Washington, D. C., 1989.

Roden, G. I., On nonseasonal temperature and salinity variations along the west coast of the United States and Canada, *CALCofi Rep.*, 8, pp. 95–119, Calif. Coop. Oceanic Fish. Invest., Mar. Life Res. Group, Scripps Inst. of Oceanogr., La Jolla, 1961.

Roos, M., Possible climate change and its impact on water supply in California, paper presented at Oceans '89 Conference, Inst. of Electr. and Electron. Eng., Seattle, Wash., Sept. 18–21, 1989.

Scheuring, A. F. (Ed.), *A Guide Book to California Agriculture*, University of California Press, Berkeley, 1983.

Siegfried, C. A., M. E. Kopache, and A. W. Knight, The benthos of a portion of the Sacramento River (San Francisco Bay Estuary) during a dry year, *Estuaries*, 3, 296–307, 1980.

Trenberth, K. E., and D. A. Paolino, The northern hemisphere sea-level pressure data set: Trends, errors, and discontinuities, *Mon. Weather Rev.*, 108, 855-872, 1980.

U.S. Bureau of Reclamation, Water development: Central Valley/Delta, document for State of Calif. Water Resour. Control Board's Bay/Delta Hearings, 45 pp.. Sacramento, 1987.

Walters, R. A., and J. W. Gartner, Sub-tidal sea level and current variations in the northern reach of San Francisco Bay, *Estuarine Coastal Shelf Sci.*, 21, 17–32, 1985.

Woodruff, S. D., R. J. Slutz, R. L. Jenne, and P. M. Steurer, A Comprehensive Ocean-Atmosphere Data Set, *Bull. Am. Meteorol. Soc.*, 68, 1239–1250, 1987.

D. R. Cayan, U.S. Geological Survey, Scripps Institution of Oceanography, La Jolla, CA 92093.

D. H. Peterson, U.S. Geological Survey, MS-496, Menlo Park, CA 94025.

(Received October 10, 1991;
revised August 27, 1992;
accepted September 8, 1992.)